

Multi-modal classification of forest biodiversity potential from 2D orthophotos and 3D airborne laser scanning point clouds

Simon B. Jensen^{a,b,*}, Stefan Oehmcke^{b,c,d}, Andreas Møgelmoose^{a,b}, Meysam Madadi^e,
Christian Igel^{b,c}, Sergio Escalera^{a,b,e}, Thomas B. Moeslund^{a,b}

^a*Visual Analysis and Perception Laboratory,, Aalborg University, Denmark*

^b*Pioneer Centre for Artificial Intelligence, Denmark*

^c*Department of Computer Science, Copenhagen University, Denmark*

^d*Institute for Visual & Analytic Computing, Rostock University, Germany*

^e*University of Barcelona and Computer Vision Center, Spain*

Abstract

Accurate assessment of forest biodiversity is crucial for ecosystem management and conservation. While traditional field surveys provide high-quality assessments, they are labor-intensive and spatially limited. This study investigates whether deep learning-based fusion of close-range sensing data from 2D orthophotos (12.5 cm resolution) and 3D airborne laser scanning (ALS) point clouds (8 points/m²) can enhance biodiversity assessment. We introduce the BioVista dataset, comprising 44 378 paired samples of orthophotos and ALS point clouds from temperate forests in Denmark, designed to explore multi-modal fusion approaches for biodiversity potential classification. Using deep neural networks (ResNet for orthophotos and PointVector for ALS point clouds), we investigate each data modality's ability to assess forest biodiversity potential, achieving mean accuracies of 69.4% and 72.8%, respectively. We explore two fusion approaches: a confidence-based ensemble method and a feature-level concatenation strategy, with the latter achieving a mean accuracy of 75.5%. Our results demonstrate that spectral information from orthophotos and structural information from ALS point clouds effectively complement each other in forest biodiversity assessment.

Keywords: Close-range sensing, Orthophotos, Airborne Laser Scanning (ALS), Deep Learning, Multi-modal fusion, Forest biodiversity

*Corresponding author. Email: sbje@create.aau.dk

1. Introduction

1.1. Background and motivation

Forest biodiversity is under significant threat due to human activities such as deforestation, habitat fragmentation and climate change (Aerts and Honnay, 2011; FAO and UNEP, 2020). The biodiversity is fundamental to forest ecosystem functioning which supports processes that are crucial to human and animal well-being, such as nutrient cycling, carbon sequestration, water regulation, and soil formation (Goldstein et al., 2020; Thompson et al., 2009).

Recent regional and international initiatives such as the EU Biodiversity strategy for 2030 (European Commission, 2020) and the United Nations Strategic Plan for Forests under the Paris agreement and the Sustainable Development Goals (SDGs) (United Nations Department of Economic and Social Affairs, 2021, 2017) aim to increase protected forest areas and enhance forest biodiversity. However, to effectively prioritize conservation efforts and resources, scalable methods for identifying high biodiversity priority areas are essential (Kerry et al., 2022).

1.2. Current assessment methods and limitations

Traditional forest biodiversity assessment methods rely heavily on resource-intensive manual fieldwork. Established approaches like the Forest Health Monitoring Program in the United States (Potter and Conkling, 2022), the RAINFOR Amazon Forest Inventory Network methodology in South America (Malhi et al., 2002) and the International Co-operative Program on Assessment and Monitoring of Air Pollution Effects on Forests in Europe (Michel et al., 2022) provide valuable qualitative insights through detailed ground surveys. However, these methods are limited in their spatial and temporal coverage due to the intensive nature of manual tree measurement, plant identification, and habitat assessment protocols. As a result, large-scale biodiversity assessments often rely on extrapolation from sparse sample plots (Kangas et al., 2018).

1.3. Remote sensing approaches

Remote sensing and close-range remote sensing data, which observes targets at distances ranging from non-contact short range up to several hundred meters, combined with recent advancements in deep learning (LeCun et al., 2015) offers promising capabilities for rapid and large-scale forest assessment.

LiDAR-based assessment of forest structural characteristics like aboveground biomass is a well-established field (Knapp et al., 2020; Magnussen et al., 2018; Pan et al., 2013). Recent deep learning approaches have also shown improved performance in extracting forest-related variables, such as tree counting, tree height prediction, biomass estimation and forest canopy cover estimation directly from various remote sensing imagery (Cheng et al., 2024; Liu et al., 2023; Li et al., 2023; Reiner et al., 2023; Yuan et al., 2020; Brandt et al., 2018; Kussul et al., 2017), see Brandt et al. (2024) for a review.

However, the integration of spectral information from optical sensors with structural information from LiDAR remains an underexplored avenue with significant potential for comprehensive forest assessment (Kangas et al., 2018). A study by Zhang et al. (2019) demonstrated the potential of this combination by learning models that predict above-ground biomass from Landsat 8 imagery in combination with ALS data. Their approach relied on deriving statistical features from the optical and LiDAR datasets, which served as inputs to the models. While effective to some extent, such features often fail to capture the fine-grained structural complexities and interactions present in LiDAR data (as shown by Oehmcke et al. (2024)). This underscores the need for models that operate directly on both, 2D and 3D data, enabling them to learn richer representations without being constrained by hand-crafted features.

1.4. 2D and 3D fusion

Fusion of 2D- and 3D data presents unique technical challenges due to their fundamentally different data structures. While 2D images are dense, ordered and discrete, 3D LiDAR point clouds are sparse, order-less and continuous (Cui et al., 2022). In recent years, 2D and 3D data fusion has become an emergent research theme in e.g., autonomous vehicles in order to achieve robust 3D object detection and semantic segmentation. Although LiDAR-only methods have achieved impressive results in 3D object detection (Yang et al., 2020; Shi et al., 2019), they

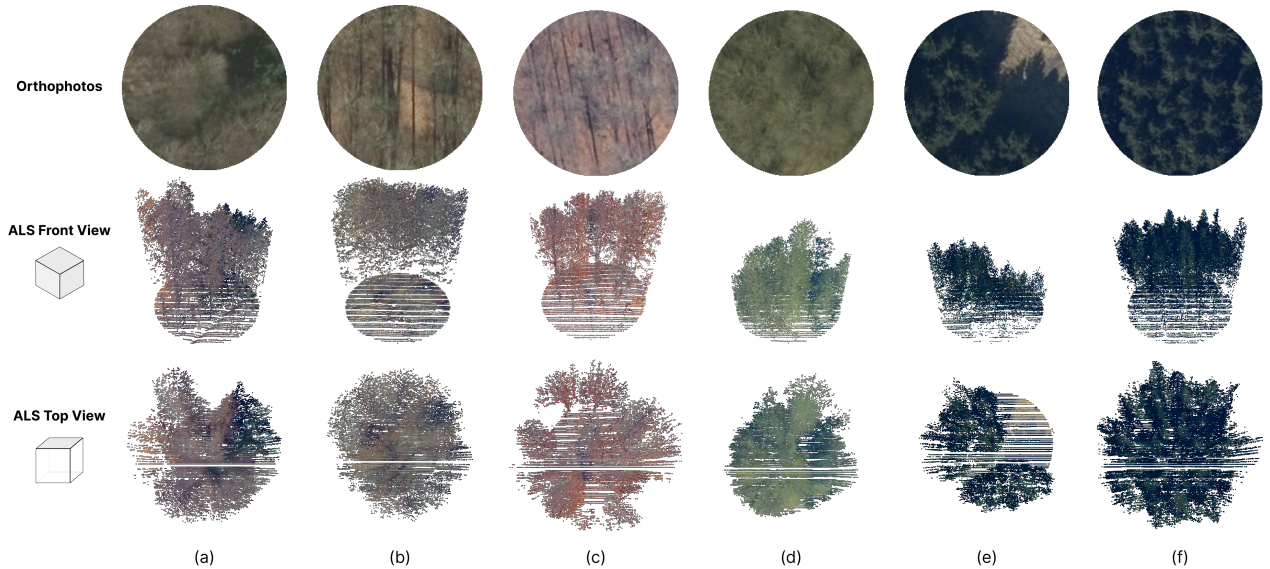


Figure 1: Sample visualization. Paired examples of 2D orthophotos and 3D airborne laser scanning (ALS) point cloud samples from the BioVista dataset, showing both front and top views of point clouds. Examples (a), (b), and (c) represent high biodiversity potential forest class while (d), (e), and (f) represent low biodiversity potential forest class.

often struggle with data sparsity, particularly for distant objects which inevitably have lower sampling density in the scans. Multi-modal approaches that leverage both dense 2D images and 3D LiDAR point clouds have shown increasing promise and recent work suggests that multi-modal approaches are gaining an edge (Wu et al., 2023; Yoo et al., 2020), although the definitive superiority of either paradigm remains an open research question.

1.5. Research objectives and contributions

This study investigates how 2D and 3D close-range remote sensing data complement each other for assessing forest biodiversity potential. We introduce the BioVista dataset - a comprehensive collection of paired orthophotos and airborne laser scanning (ALS) point clouds from temperate forests in Denmark, labeled for biodiversity potential. Examples of orthophotos and ALS point cloud pairs are seen in Figure 1. Denmark offers an ideal setting for creating such a dataset due to its long-standing tradition of detailed forest monitoring (Nord-Larsen et al., 2023), comprehensive geographic data collection, and open data policies (Hansen et al., 2011).

We summarize the contributions of this work as follows:

- **The BioVista dataset:** Development the BioVista dataset, containing 44 378 pairs of 2D orthophotos and 3D ALS point clouds, labeled as high- or low biodiversity potential forest. This dataset and the associated annotations are made publicly available and provide a valuable resource for close-range remote sensing-based forest assessment tasks.
- **Evaluation of deep learning approaches:** We test the forest biodiversity assessment potential of deep learning-based methods, on the BioVista dataset, using either 2D orthophotos or 3D ALS point clouds as inputs.
- **Multi-modal fusion:** We evaluate two multi-modal fusion methods combining spectral and structural information from 2D orthophotos and 3D ALS point clouds – confidence ensembling (late fusion) and feature concatenation (feature-level fusion) on the BioVista dataset.

The insights and methodologies developed through this research contribute to the broader goal of developing efficient, scalable approaches for forest biodiversity assessment and monitoring using close-range sensing technologies.

The remainder of this paper is organized as follows: Section 2 presents the BioVista dataset, including data collection, preprocessing and preparation. Section 3 details our deep learning methodology, covering both single-modality approaches (2D orthophoto and 3D ALS point cloud classification) and multi-modal fusion strategies. Section 4 presents our experimental results and performance analysis. Section 5 discusses limitations and potential improvements of our approach, while Section 6 concludes with key findings and future research directions.

2. Dataset

2.1. The BioVista dataset

The BioVista dataset, introduced in this study, combines High Nature Value (HNV) proxies (Johannsen et al., 2015), described in detail in Section 2.2, with remote sensing data to create a comprehensive resource for forest biodiversity potential classification. The dataset is a unique, high-quality resource for forest assessment, made possible by Denmark’s tradition of comprehensive forest registries (Nord-Larsen et al., 2023), extensive geographic data collection, and open data policies (Hansen et al., 2011).

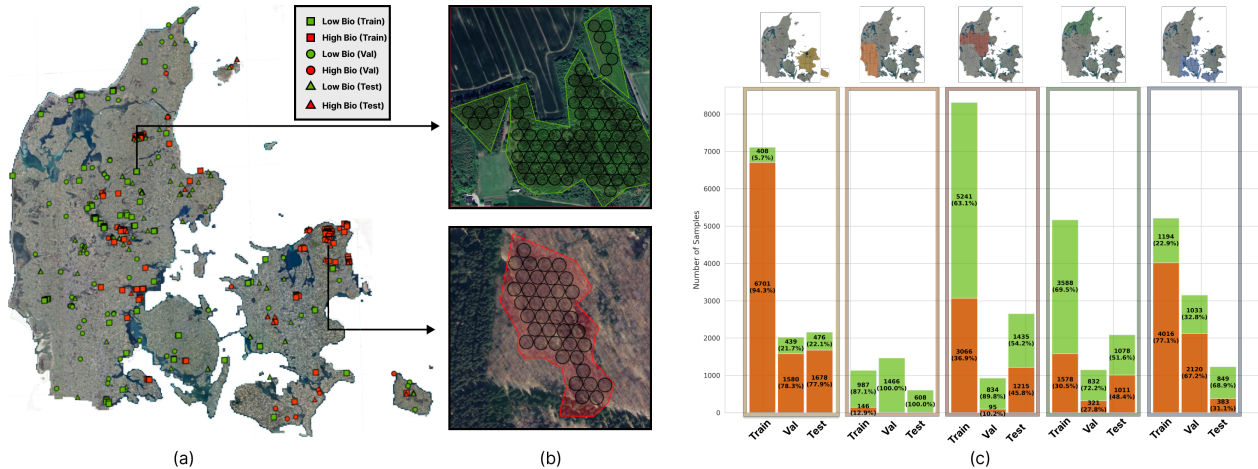


Figure 2: Dataset structure. Geographic distribution of forest patches and sampling methodology. (a) Forest patches used for sampling training, validation and test samples from Denmark. (b) Example of non-overlapping circular samples (30-meter diameter) extracted from a forest patch. (c) Distribution plot showing class representation across train, validation and test sets by region.

The dataset comprises 44 378 pairs of 2D orthophoto images and 3D ALS point clouds derived from forests in Denmark, labeled as either high- or low biodiversity potential. An overview of the dataset and geographic location of forest patches can be seen in Figure 2. The orthophotos and point clouds in the BioVista dataset, have a circular shape with a diameter of 30 meters as seen in Figure 1. This shape and size conforms to the test plot standard used in e.g., the National Forest Inventory (NFI) of Denmark (Alban et al., 2019), and is very similar to other National Forest Inventory (NFI) standards (Kangas et al., 2018). One sample covers an area of $\sim 707m^2$ and the rationale is to have a large enough area to include a diverse selection of both small and larger trees and vegetation within a single sample, as well as variations in soil, ground cover, and other ecological factors within the same area.

2.2. Biodiversity ground truths

We use the HNV forest map (Johannsen et al., 2015), seen in Figure 3, as the foundation for gathering ground truth labels for our samples. The HNV forest map is based on 11 features that serve as proxies for forest biodiversity potential, combining historical and current data to provide a comprehensive assessment. Proxy features include among others canopy height variation, coastal proximity, tree- and plant richness, canopy cover, occurrence of large trees, and occurrence of inner forest edges. Examples of proxy features are seen in Figure 4. Each

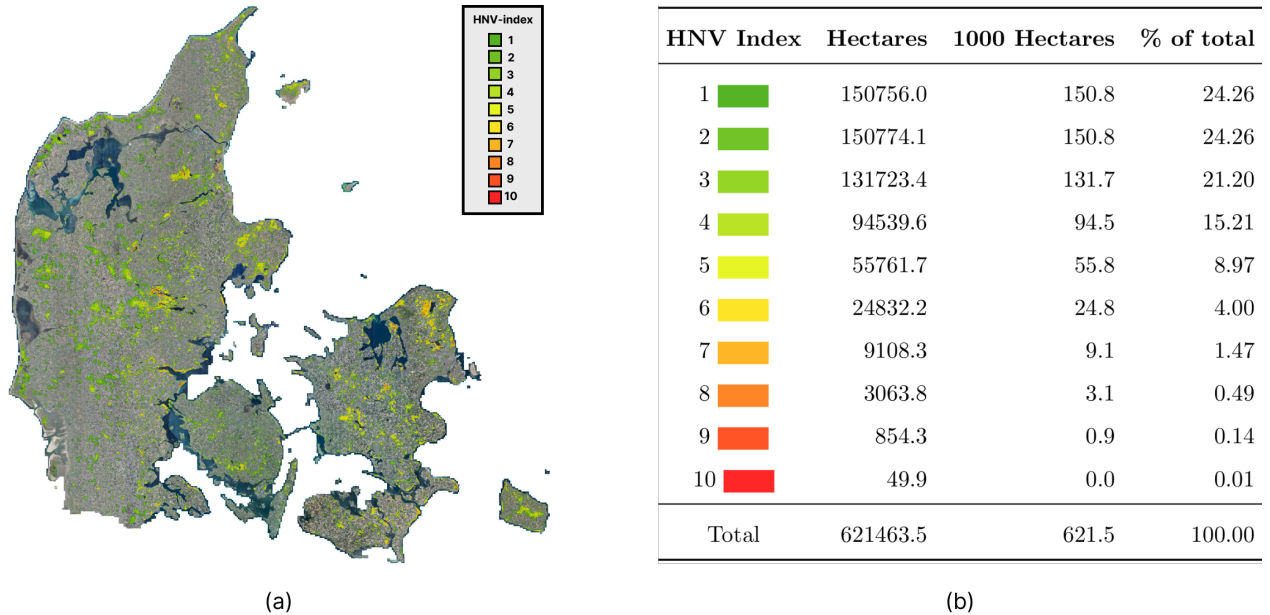


Figure 3: HNV forest distribution. High Nature Value (HNV) forest map of Denmark (Johannsen et al., 2015). (a) Spatial distribution where scores from 1 (low biodiversity potential) to 10 (high biodiversity potential) are indicated by color gradients from green to red. (b) Quantitative distribution showing that forest areas with HNV-indices 1-3 comprise nearly 75% of Danish forests, while areas with indices 8-10 represent less than 1%.

forest area is given a score from 0 to 11, where 0 is a very low nature value score which is indicated by green colors and 11 is a very high nature value score indicated by red colors. Only a small sub-set of forest areas achieve a score of 10, no forest achieves a score of 11. See Figure 3 for the distribution of HNV-indices. Although the color scheme may appear counterintuitive, with green representing lower biodiversity values and red representing higher ones, we choose to maintain consistency with the original HNV forest map convention.

2.3. Dataset creation process

To create a clear distinction in our forest biodiversity potential classification task, we define low biodiversity potential forests as those with an HNV-index of 1-3 and high biodiversity potential forests as those with an HNV-index of 8-10, while ignoring forest with HNV-index between 4 and 7. This approach simplifies the classification problem and allows for a more focused comparison of classifiers trained on orthophotos, ALS point clouds, and a combination of the two.



Figure 4: Biodiversity indicators. Visual examples of HNV proxy features used for forest biodiversity assessment: (a) big trees, (b) coastal proximity, (c) canopy cover, and (d) plant richness. Photo credits: (a) Bettina Nygaard, (b,d) Henriette Bjerregaard, (c) Peter Wind.

The dataset creation process involves the following steps:

1. Filtering the HNV forest map (seen in Figure 3) to include only forest patches with indices 1-3 and 8-10, used for extracting low biodiversity forest potential samples and high biodiversity forest potential samples, respectively.
2. Filtering narrow forest patches using morphological opening and exclude forest patches with an area below 0.5 hectares using connected components analysis, thereby following the minimum forest size definition of FAO and UNEP (2020).
3. Randomly selecting low biodiversity potential forest patches and high biodiversity potential forest patches. See Figure 2 for an overview of the randomly selected forest patches.
4. Converting the randomly selected forest patches to polygons using QGIS (QGIS Geographic Information System).
5. Extracting coordinates for non-overlapping samples from each forest patch polygon.
6. Downloading 2D orthophotos and 3D ALS point clouds for the sample coordinates, while ensuring temporal consistency between the orthophotos and ALS point clouds as described in Section 2.6.

2.4. Dataset split

We randomly split the samples into training, validation and test sets, with a 60%-20%-20% ratio. The location of training, validation and test forest patches can be seen in Figure 2. The resulting split and distribution of high- and low biodiversity potential forest polygons and samples is shown in Table 1.

Table 1: Dataset distribution. Distribution of forest samples across the training-, validation- and test sets, showing the number of polygons, number of samples, average samples per polygon, and average polygon size in hectares for both high- and low biodiversity potential forests.

	Category	# Polygons	# Samples	Avg. samples	Avg. size (ha)
Train	High Bio. Potential	88	15 507	176.2	19.9
	Low Bio. Potential	95	11 418	120.2	13.8
Val	High Bio. Potential	16	4116	257.3	28.7
	Low Bio. Potential	58	4604	79.4	10.1
Test	High Bio. Potential	41	4287	104.6	12.2
	Low Bio. Potential	78	4446	57.0	7.6
Total		376	44 378	118.0	16.1

2.5. 2D orthophotos

The 2D orthophotos used in this project are derived from yearly nationwide aerial photography of Denmark and are part of GeoDanmark’s geographic administration framework (GeoDanmark, 2024). Orthophotos are created by adjusting each pixel according to the camera’s position and the elevation model of the Earth’s surface, ensuring that the images are geometrically corrected and can be used for precise measurements.

The orthophotos have a ground resolution of 12.5 cm per pixel. The orthophotos are captured annually before leaf-out, between March 1st and May 1st and the images undergo extensive post-processing to ensure consistent colors, contrast, and brightness across the entire yearly captured data. The resulting map of Denmark, from the 2023 orthophoto collection, can be seen in Figure 5.

2.6. 3D ALS point clouds

The 3D ALS point clouds used in this study is part of the Danish Height Model dataset (Klimadatastyrelsen, 2024). This comprehensive dataset covers the entire country of Denmark and is continuously updated through yearly systematic airborne laser scanning. As of 2018 and forward, 1/5 of the country is updated annually. In this research we use ALS point clouds from 2019, 2020, 2021, 2022 and 2023 depending on the area of the forest, as illustrated in

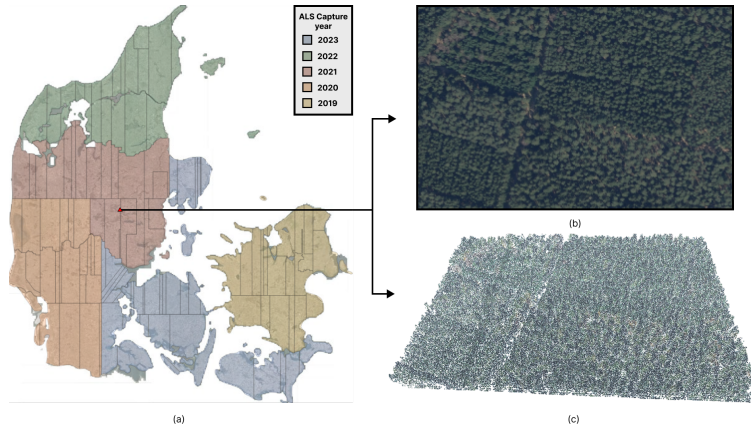


Figure 5: Data sources. Orthophotos and ALS point cloud coverage of Denmark. (a) 2023 orthophoto map with ALS capture dates overlaid. (b) High-resolution orthophoto example (56.161144°N, 9.594725°E). (c) Corresponding ALS point cloud.

Figure 5. For each forest area, we ensure temporal consistency by using orthophotos captured in the same year as the corresponding ALS point cloud data, allowing for fair comparison between the two modalities and ensuring that both data sources represent the forest conditions from the same time period. The point clouds are available in tiles spanning 1×1 km and the point density averages 8 points/m² for data, with a horizontal accuracy of 0.15 m and a vertical accuracy of 0.05 m.

3. Method

In this section, we describe our methodology for assessing forest biodiversity potential using deep learning approaches. We explore four distinct classification methods: 2D orthophoto classification using ResNet, 3D ALS point cloud classification using PointVector (Deng et al., 2023) and two fusion approaches that combine these modalities: confidence-based ensembling and feature-level concatenation, as illustrated in Figure 6.

3.1. 2D orthophoto image classification

For the classification of forest biodiversity potential using 2D orthophotos, we employ the ResNet architecture (He et al., 2015). ResNet is a deep convolutional neural network (CNN) architecture known for its ability to train effectively by using residual connections to mitigate the vanishing gradient problem. The architecture is well-suited for image classification tasks

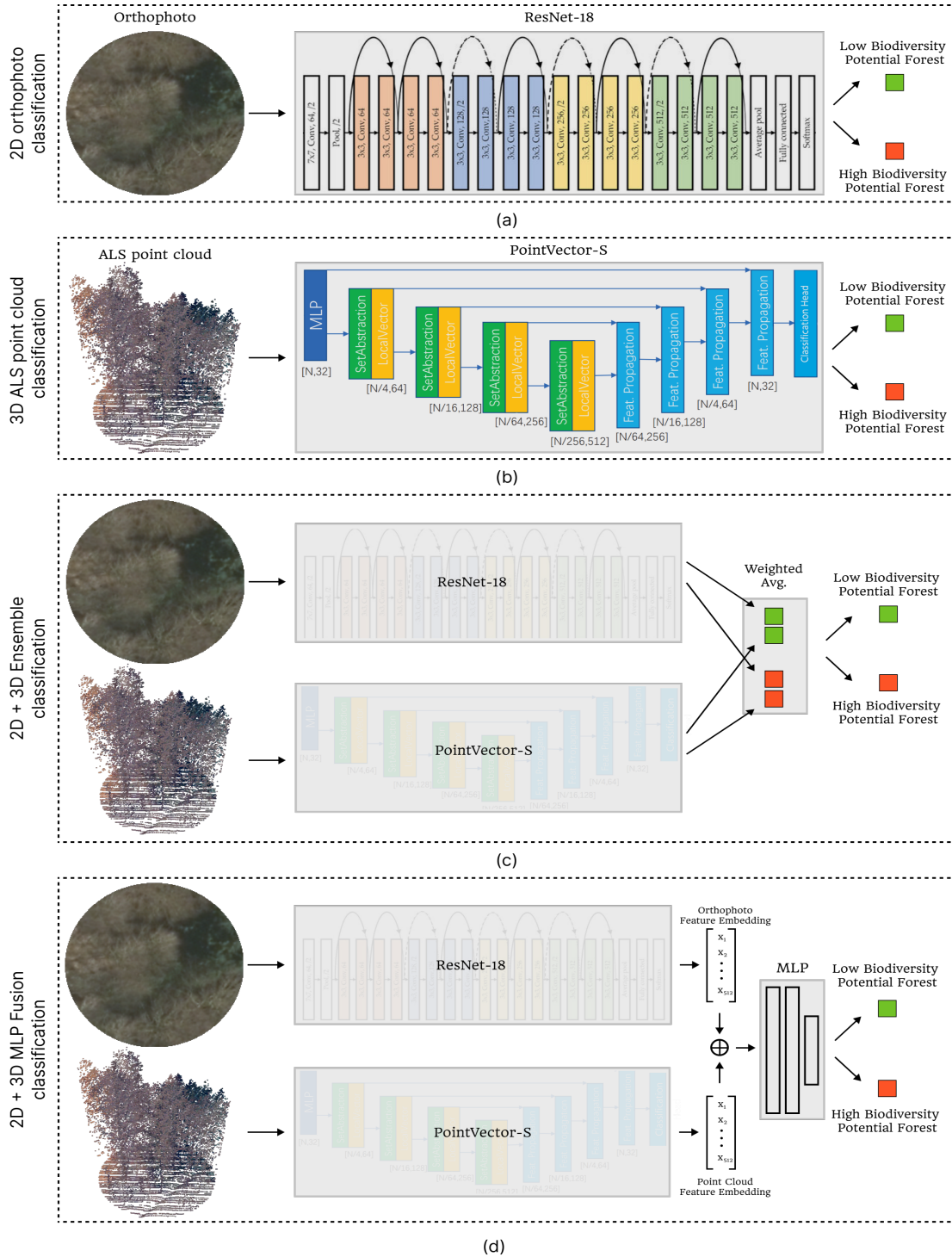


Figure 6: Classification approaches. Architectural overview of the four classification approaches: (a) 2D orthophoto classification using ResNet-18, (b) 3D ALS point cloud classification using PointVector-S, (c) 2D + 3D Ensemble classification combining prediction probabilities through weighted averaging and (d) 2D + 3D MLP Fusion integrating feature embeddings from both modalities via concatenation.

where the model must learn complex patterns from large-scale image datasets. A ResNet consists of a combination of convolutional layers, batch normalization, and ReLU activation functions, followed by fully connected layers.

3.2. 3D ALS point cloud classification

For the task of classifying the biodiversity potential of forests based on 3D ALS point clouds, we employ the PointVector architecture (Deng et al., 2023). The architecture was proposed in a small, large and x-large version, and we utilize a variation of the small model, PointVector-S. PointVector is a state-of-the-art point cloud processing model that introduces a novel vector-oriented point set abstraction module to enhance local feature aggregation, allowing for more effective extraction of spatial information from point cloud data. PointVector builds upon previous successful point-based networks like PointNet++ (Qi et al., 2017) and PointNeXt (Qian et al., 2022). The PointVector model has demonstrated SOTA performance on various 3D point cloud benchmarks such as S3DIS (Armeni et al., 2016) and ScanObjectNN (Uy et al., 2019), while using significantly fewer parameters than comparable models, as shown by OpenTrech3D (Hansen et al., 2024).

3.3. 2D-3D multi-modal classification

One challenge in combining 2D orthophotos and 3D ALS point clouds for classification is their fundamentally different data structures. Images are regular, ordered and discrete while point clouds are irregular, order-less and continuous. These differences has led to different feature extraction methodologies, as presented in Section 3.1 and 3.2 and shown in Figure 6. To address this challenge and leverage the complementary information from both modalities, we explore two distinct fusion approaches: confidence ensembling and feature concatenation.

3.3.1. Confidence ensembling

Our first fusion approach utilizes a confidence-based ensemble method that combines the output probabilities from trained ResNet and PointVector classifiers. For each input sample, we obtain classification probabilities from both models and combine them using a weighted average:

$$P(\text{class} \mid \text{input}) = w_{2D} \cdot P_{2D}(\text{class} \mid \text{input}) + w_{3D} \cdot P_{3D}(\text{class} \mid \text{input}) \ ,$$

where P_{2D} and P_{3D} are the class probabilities from the ResNet and PointVector models respectively, and w_{2D} and w_{3D} are the corresponding weights. The weights are determined through validation set performance, with the final prediction being the class with the highest combined probability. This approach, which can be viewed as a simple form of stacked generalization (Wolpert, 1992), allows each model to contribute according to its relative strength in classification, while maintaining the independence of the 2D and 3D processing pipelines.

3.3.2. MLP fusion

Our second fusion approach explores a more integrated strategy by concatenating feature embeddings from the trained 2D and 3D models. This method combines the rich spectral information captured by ResNet-18’s image features with the structural information encoded in PointVector-S’s point cloud features, as shown in Figure 6. The process involves:

- Extracting 512-dimensional feature vectors from ResNet-18 and PointVector-S.
- Concatenating feature vectors to create a 1024-dimensional combined feature vector.
- Processing the combined features through a Multi-Layer Perceptron (MLP) classifier.

The MLP architecture consists of 1024 nodes (512 from ResNet-18 + 512 from PointVector-S), three hidden layers with sizes: 1024, 1024, 512, followed by ReLU activation functions after each hidden layer.

We freeze the weights of both the ResNet-18 and PointVector-S models, using them only as feature extractors. This approach ensures that the pre-trained models maintain their learned representations while allowing the MLP to learn higher-level feature interactions.

4. Experiments

To evaluate the effectiveness of our proposed methods for classifying forest biodiversity potential using remote sensing data, we conducted a series of experiments using the BioVista dataset. Our experiments aimed to compare the performance of 2D orthophoto-based classification, 3D ALS point cloud-based classification, and fusion approaches that combine both data modalities.

4.1. Evaluation metrics

We track the overall accuracy and the mean accuracy for assessing the performance of the various classifiers’ ability to correctly identify high- and low biodiversity potential forests.

Overall accuracy (OAcc) is the most straightforward measure of a classifier’s performance. It is defined as the ratio of correctly classified samples, N_{correct} , to the total number of samples, N_{total} :

$$\text{OAcc} = N_{\text{correct}}/N_{\text{total}}$$

While OAcc provides a general sense of the model’s performance, it can be misleading in cases of class imbalance. Mean accuracy (MAcc) addresses the potential bias in overall accuracy due to class imbalance and is calculated as the average of the accuracies for each class, thereby, weighing the significance of each class equally important. For BioVista we calculated the accuracy for classifying low biodiversity potential forest, Acc_{low} and accuracy for classifying high biodiversity potential forest, Acc_{high} and define the MAcc as follows:

$$\text{MAcc} = \frac{\text{Acc}_{\text{high}} + \text{Acc}_{\text{low}}}{2}$$

4.2. Model performance evaluation

4.2.1. 2D classification

For the classification of forest biodiversity potential using 2D orthophotos, we employed the ResNet-18 architecture (He et al., 2015). While deeper variants such as ResNet-34 and ResNet-50 were explored in preliminary experiments, they did not yield significant performance improvements, leading us to select the more computationally efficient ResNet-18. This architecture outputs feature vectors of size 512, matching the dimensionality of our PointVector-S model’s output, which proved advantageous for our fusion experiments.

To enhance model robustness and prevent over-fitting, we implemented several data augmentation techniques during training:

- Random horizontal and vertical flipping and random rotation up to 45 degrees to account for rotational invariance in aerial imagery.
- Color jittering with brightness, saturation, and hue adjustments to account for varying lighting conditions at capture times.

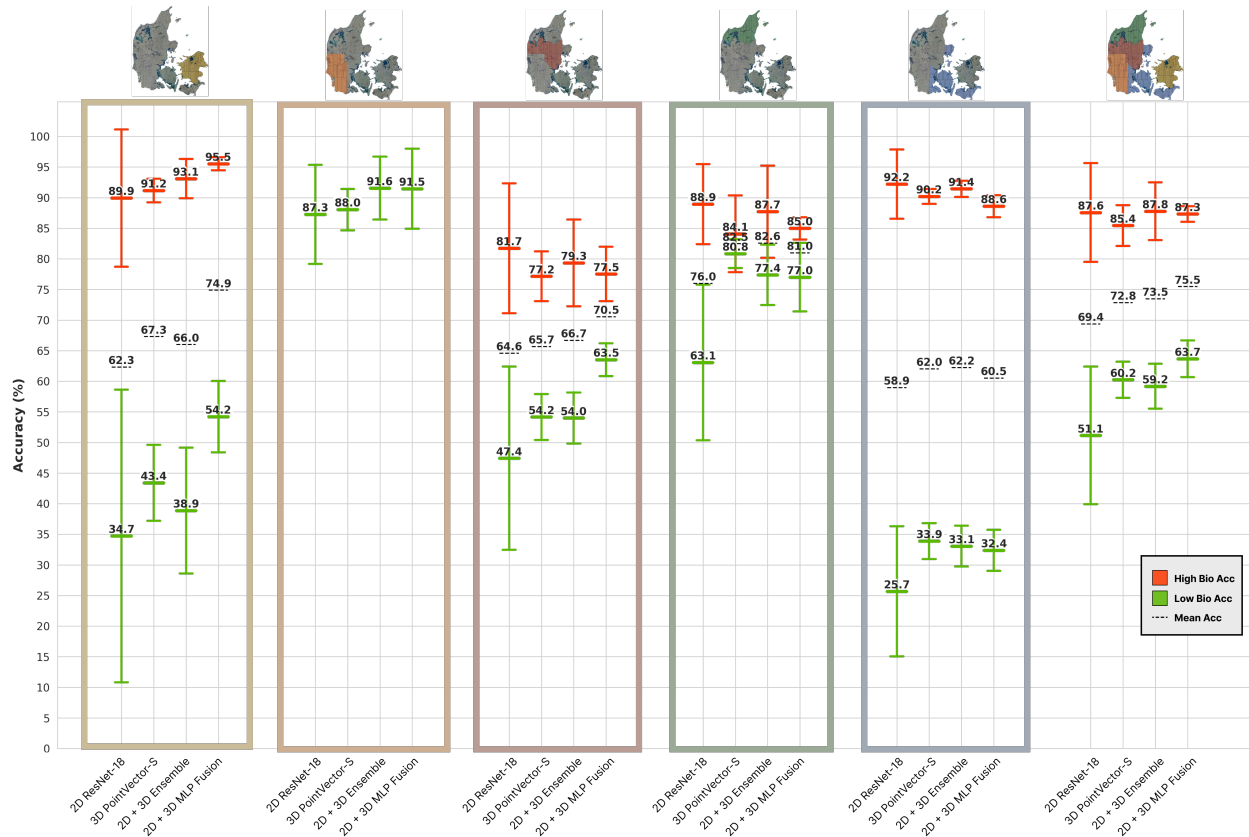


Figure 7: Regional model performance. Mean test accuracy per class across different regions for each classification model. Results show average performance across 5 runs with standard deviations.

The network was initialized with random weights rather than ImageNet pre-training, as the aerial perspective and characteristics of orthophotos differ substantially from natural images.

The model was trained for 100 epochs using the Adam optimizer with a learning rate of 0.001 and a batch size of 32. Input images were preprocessed to a resolution of 240×240 pixels, maintaining the original 12.5 cm ground sampling distance. For circular sample areas, pixels outside the 30-meter diameter circle were masked to zero to ensure the model focused only on the relevant forest area.

When averaged over five runs, ResNet-18 achieved an overall accuracy of $69.0\% \pm 3.7\%$ and a mean accuracy of $69.4\% \pm 3.7\%$ on the test set, as seen in Figure 7 and Table 2. The model performed notably better on high biodiversity potential forests ($87.6\% \pm 8.0\%$) compared to low biodiversity potential forests ($51.2\% \pm 11.3\%$), indicating a class imbalance in the model’s predictive capabilities.

Table 2: Overall model performance. The performance metrics of the four different classification models on the test data, including overall accuracy (OAcc), mean accuracy (MAcc), accuracy for high biodiversity potential forests (Acc_{high}), and accuracy for low biodiversity potential forests (Acc_{low}). All metrics are reported as means with associated standard deviation across five runs.

Model	OAcc	MAcc	Acc _{high}	Acc _{low}
2D ResNet-18	69.0% ± 3.7	69.4% ± 3.7	87.6% ± 8.0	51.2% ± 11.3
3D PointVector-S	72.6% ± 0.8	72.8% ± 0.8	85.4% ± 3.4	60.2% ± 3.0
2D + 3D Ensemble	73.2% ± 1.5	73.5% ± 1.5	89.4% ± 2.9	57.6% ± 3.6
2D + 3D MLP Fusion	75.3% ± 1.1	75.5% ± 1.1	87.3% ± 1.3	63.6% ± 3.0

4.2.2. 3D classification

The PointVector-S model was trained for forest biodiversity potential classification using the ALS point cloud data. For each ALS point cloud sample, 8192 points were randomly sampled during both training, evaluation and inference to ensure consistent input size. We experimented with increasing the number of points to 16 384, but this did not yield significant performance improvements while increasing computational overhead.

Training was conducted for 10 epochs, as early experiments showed convergence after few epochs of training. We used the AdamW optimizer, similar to Deng et al. (2023) with a weight decay of 1×10^{-4} , an initial learning rate of 0.0001 and a minimum learning rate of 1×10^{-5} . The model was trained with a batch size of 8 and cross-entropy loss with label smoothing of 0.2. We used a ball query radius 0.7 meters, following the standard used by Jensen et al. (2023).

During training, we applied the same data augmentation techniques as (Qian et al., 2022), which include:

- Random rotation around the z-axis (up to 360 degrees).
- Random scaling between 0.9 and 1.1.
- Random point jittering with sigma=0.005 and clip=0.02.
- XYZ alignment with gravity dimension set to the z-axis.

The model achieves a mean accuracy of $72.8\% \pm 0.8\%$ and an overall accuracy of $72.6\% \pm 0.8\%$ on the test set, when averaged across 5 runs, thereby slightly outperforming the 2D classifier, as seen in Figure 7 and Table 2. The PointVector architecture’s vector-oriented point set abstraction module proved effective at aggregating local geometric features from the irregularly sampled LiDAR points, suggesting that 3D structural information from ALS point clouds provides valuable cues for biodiversity potential assessment.

4.2.3. 2D-3D classification

For the fusion of 2D orthophoto and 3D ALS point cloud data, we implemented two distinct approaches: a confidence-based ensemble model and an MLP-based feature fusion model as covered in Section 3.

The ensemble model combines prediction probabilities through weighted averaging, with weights determined through validation set performance. No additional training is required for this approach, as it directly uses the outputs from the independently trained models.

For the MLP fusion model, we extracted 512-dimensional feature vectors from both the trained ResNet-18 and PointVector-S models, which were frozen during the fusion training process. Training was conducted for 10 epochs using the Adam optimizer with a learning rate of 1×10^{-6} and a batch size of 128.

The ensemble approach achieved an overall accuracy of $73.2\% \pm 1.5\%$ and a mean accuracy of $73.5\% \pm 1.5\%$ on the test set, showing particularly strong performance on high biodiversity potential forests ($89.4\% \pm 2.9\%$). The MLP fusion model demonstrated the best overall performance among all approaches, with an overall accuracy of $75.3\% \pm 1.1\%$ and a mean accuracy of $75.5\% \pm 1.1\%$. Notably, the MLP fusion achieved more balanced performance across classes, with $87.3\% \pm 1.3\%$ accuracy on high biodiversity potential forests and $63.6\% \pm 3.0\%$ accuracy on low biodiversity potential forests, as shown in Figure 7 and Table 2.

4.3. Qualitative analysis

To better understand the models’ behavior, we analyze their predictions on two representative forest patches with contrasting biodiversity potential in Figures 8 and 9. Figure 8 shows predictions on a low biodiversity potential forest patch (id: low_2021_76) containing 142

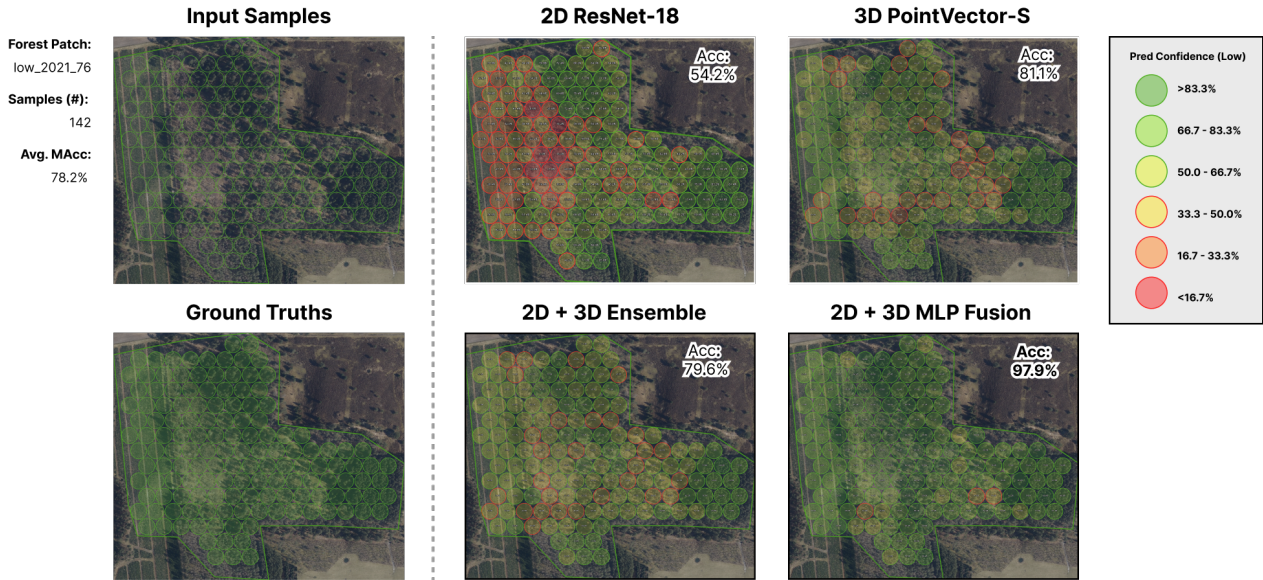


Figure 8: Low biodiversity case study. Prediction results from all four models on a low biodiversity potential forest patch (low_2021_76). Sample predictions shown with colored borders (red: high biodiversity potential, green: low biodiversity potential) and confidence scores. The MLP Fusion approach achieves superior performance compared to single-modality methods.

samples. The MLP Fusion approach notably outperforms single-modality methods, achieving 97.9% mean accuracy compared to ResNet’s 54.2% and PointVector’s 81.0%. The confidence scores, indicated by color intensity, show that the MLP Fusion approach makes more decisive and accurate predictions, particularly in areas where ResNet struggles with false positives.

The Ensemble method (79.6% accuracy) performs similarly to PointVector, suggesting that simple confidence averaging does not fully capture the complementary strengths of the two modalities. Figure 9 demonstrates a consistent pattern across all models when analyzing a high biodiversity potential forest patch (high_2022_20). The models show a systematic bias in their predictions based on tree species composition – samples dominated by broad-leaf trees are typically classified as high biodiversity potential, while those containing primarily conifer trees are predicted as low biodiversity potential. This behavior reveals a limitation in the models’ understanding of biodiversity potential, as they appear to over-rely on tree species composition rather than considering other structural and ecological factors. In this patch, the performance differences between models are less pronounced (ranging from 75.4% to 81.5% accuracy), indicating that this systematic bias affects all approaches similarly. These

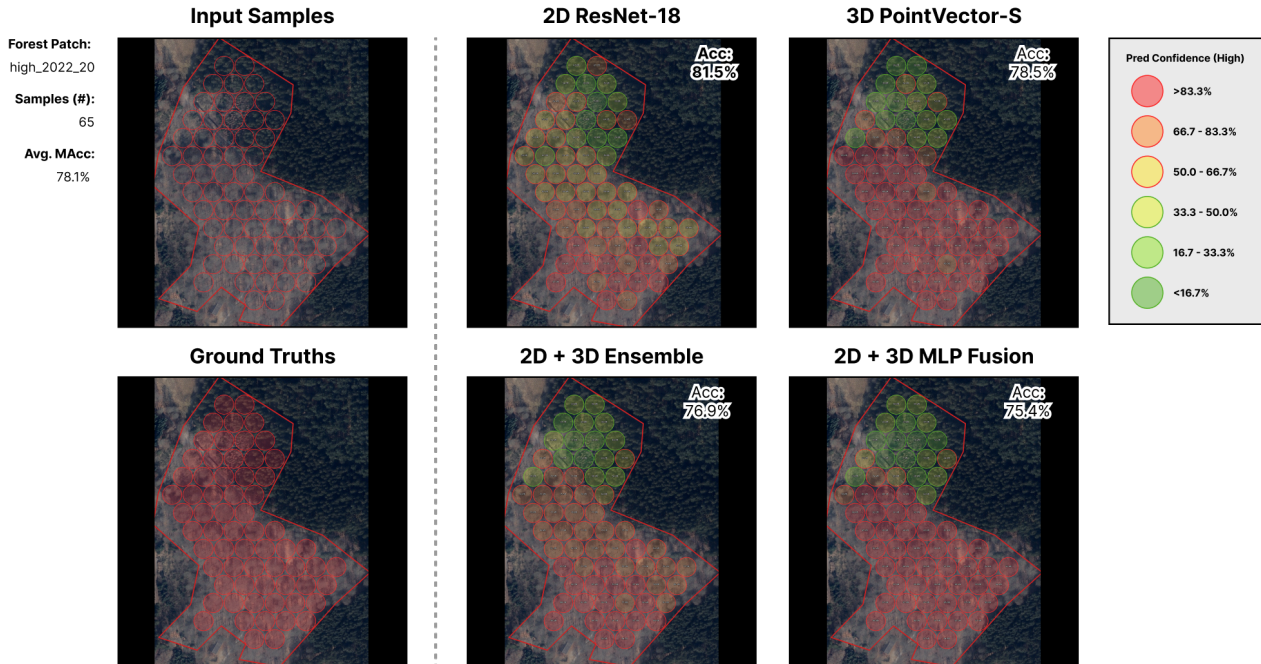


Figure 9: High biodiversity case study. Prediction results from all four models on a low biodiversity potential forest patch (high_2022.20). All models exhibit a systematic bias: classifying broad-leaf tree areas as high biodiversity potential and conifer tree areas as low biodiversity potential.

qualitative observations suggest that while our fusion approaches can significantly improve classification accuracy in some scenarios, fundamental challenges remain in capturing the full complexity of forest biodiversity potential assessment, as further discussed in Section 5.

5. Discussion

The accelerating loss of forest biodiversity represents one of the most pressing environmental challenges of our time. While traditional field-based biodiversity assessment methods provide valuable detailed insights, their resource-intensive nature makes them impractical for monitoring biodiversity at scale. Our work demonstrates that remote sensing combined with deep learning offers a promising pathway for large-scale biodiversity monitoring, though important limitations and considerations must be acknowledged.

5.1. Implications

Our results, shown in Table 2 and Figure 7 demonstrate that deep learning models can effectively assess forest biodiversity potential on a coarse-grained level using remote sensing

data, with our best model achieving a mean accuracy of 75.5%. Particularly noteworthy is how the combination of 2D orthophotos and 3D ALS point clouds enhances classification performance. The performance enhancement of the fusion approaches indicate that spectral and structural information complement each other in meaningful ways for biodiversity assessment.

However, we emphasize that these automated approaches should complement rather than replace traditional field assessments. While deep learning methods offer unprecedented scalability and efficiency, manual fieldwork remains crucial for validation, model improvement, and capturing subtleties that remote sensing might miss. The synergy between automated and manual approaches likely represents the most robust path forward for biodiversity monitoring.

5.2. Limitations

Several important limitations of our approach warrant discussion. First, we deliberately simplified the problem by focusing solely on forest structure and vegetation while excluding fauna. While this simplification was necessary for initial development, a complete biodiversity assessment would need to account for animal populations and their habitats.

The use of the HNV forest map as ground truth presents both strengths and limitations. While the map relies on proxy features rather than direct biodiversity measurements, it has undergone rigorous expert validation and systematic testing that supports its utility for identifying high-value forest areas. The temporal gap between the 2015 HNV map and more recent ALS and orthophoto data (2019-2023) initially raised concerns. We mitigated the risk of mis-classification due to the potential changes in biodiversity by excluding forests with HNV-indices between 4 and 7. Our analysis seen in Figure 7 showed consistent model performance across years, suggesting temporal robustness.

We observed interesting patterns in regional performance variations, particularly for low biodiversity potential forests. This variance likely stems from the heterogeneous nature of low biodiversity areas – these forests can exhibit various combinations of proxy features, while high biodiversity forests tend to share presence of the same proxy features.

5.3. Future work

Several promising avenues exist for improving our approach. First, exploring end-to-end training of the fusion model, rather than using frozen backbones, could potentially capture more nuanced relationships between modalities. Additionally, incorporating the available near-infrared band from orthophotos and intensity information from ALS point clouds could provide valuable additional spectral and structural information for biodiversity assessment.

A crucial next step would be testing the generalizability of our approach across different forest biomes. While our method shows promise for temperate forests in Denmark, tropical, boreal, and other forest types present distinct challenges and characteristics. Tropical forests, for instance, typically exhibit much higher species diversity and more complex canopy structures than temperate forests, which could affect both the ALS point cloud patterns and spectral signatures in orthophotos.

6. Conclusion

This study demonstrates the potential of combining 2D orthophotos and 3D ALS point clouds for automated assessment of forest biodiversity potential using deep learning. Through evaluation using our introduced BioVista dataset, we have shown that deep learning approaches can successfully classify forest biodiversity potential, with our best fusion model achieving a mean accuracy of 75.5%. The superior performance of 3D ALS point clouds compared to orthophotos, and the further improvement achieved through multi-modal fusion, suggests that combining structural and spectral information provides a more comprehensive assessment of forest biodiversity potential. While our automated approach shows promise for large-scale forest monitoring, certain limitations remain, such as systematic biases in tree species classification. Future work should explore end-to-end training of fusion models, incorporation of additional spectral and structural information, and testing across different forest biomes. This research represents a step towards developing tools that could support biodiversity conservation efforts, but further improvements in accuracy and robustness are needed before these methods could be considered for practical applications.

7. Acknowledgements and funding

This research was enabled by support and funding provided by Ambolt AI, AI Denmark and The Pioneer Centre for Artificial Intelligence (DNRF grant number P1). This work has been partially supported by the Spanish project PID2022-136436NB-I00 and by ICREA under the ICREA Academia programme. CI acknowledges support from the Danish National Research Foundation (DNRF) through the TreeSense center of excellence. The authors declare no conflict of interest.

8. CRediT authorship contribution statement

Simon B. Jensen: Conceptualization, Data curation, Methodology, Writing – original draft, Writing – review and editing. **Stefan Oehmcke:** Conceptualization, Writing – original draft, Writing – review and editing. **Andreas Møgelmoose:** Conceptualization, Writing – review and editing, Supervision. **Meysam Madadi:** Conceptualization, Writing – review and editing, Supervision. **Christian Igel:** Conceptualization, Writing – review and editing. **Sergio Escalera:** Project administration, Writing – review and editing. **Thomas B. Moeslund:** Project administration, Funding acquisition, Writing – review and editing, Supervision.

Table 3: Ensemble results. The performance metrics of the different models when using averaged predictions from five independently trained instances of each architecture, demonstrating improved stability and overall performance compared to single model results.

Model	OAcc	MAcc	Acc _{high}	Acc _{low}
2D ResNet-18	72.6%	73.0%	92.6%	53.4%
3D PointVector-S	73.7%	74.0%	87.2%	60.7%
2D + 3D Ensemble	74.1%	74.4%	89.9%	59.0%
2D + 3D MLP Fusion	76.7%	76.9%	88.1%	65.6%

Appendix A. Ensembled model performance

To ensure a fair comparison between different model architectures in our qualitative analysis, we average the predictions across five instances of each model instance to obtain a more

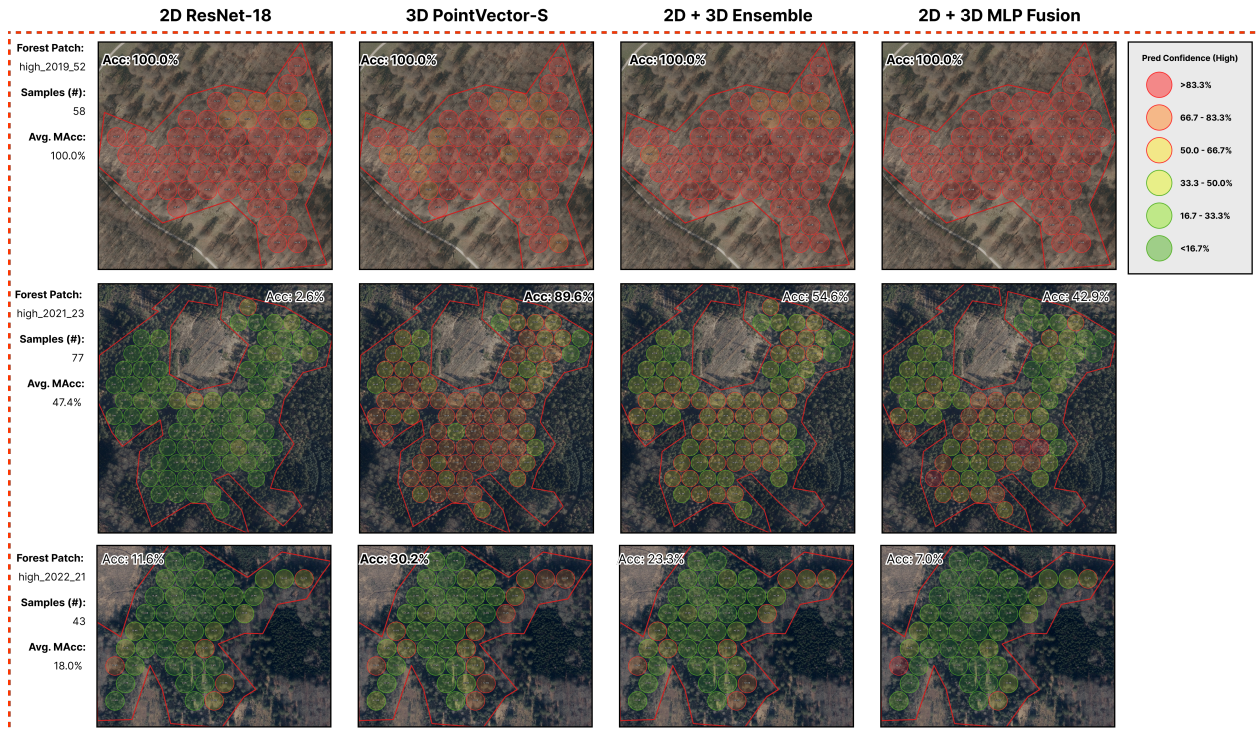


Figure B.10: High biodiversity examples. Comparison of model predictions across three high biodiversity forest patches. Sample predictions shown with colored borders indicating classification outcome and confidence levels from all four models.

representative assessment of each architecture’s capabilities. The results of these ensembled models are shown in Table 3. The 2D + 3D MLP Fusion ensemble achieves the highest performance with an overall accuracy of 76.7% and a mean accuracy of 76.9%.

Appendix B. Forest patch performance

To better understand model performance across different forest environments, we analyzed classification results on forest patches in the test set. The results are seen in Table B.4. Each forest patch represents a contiguous forest area annotated as either high- or low biodiversity. The results reveal considerable variation in model performance across different patches, with some showing perfect classification accuracy across all models while others prove challenging for all approaches.

For high biodiversity patches, we observed that several patches (e.g., high_2019_50 through high_2019_54) achieved 100% accuracy across all models, suggesting these forest areas have

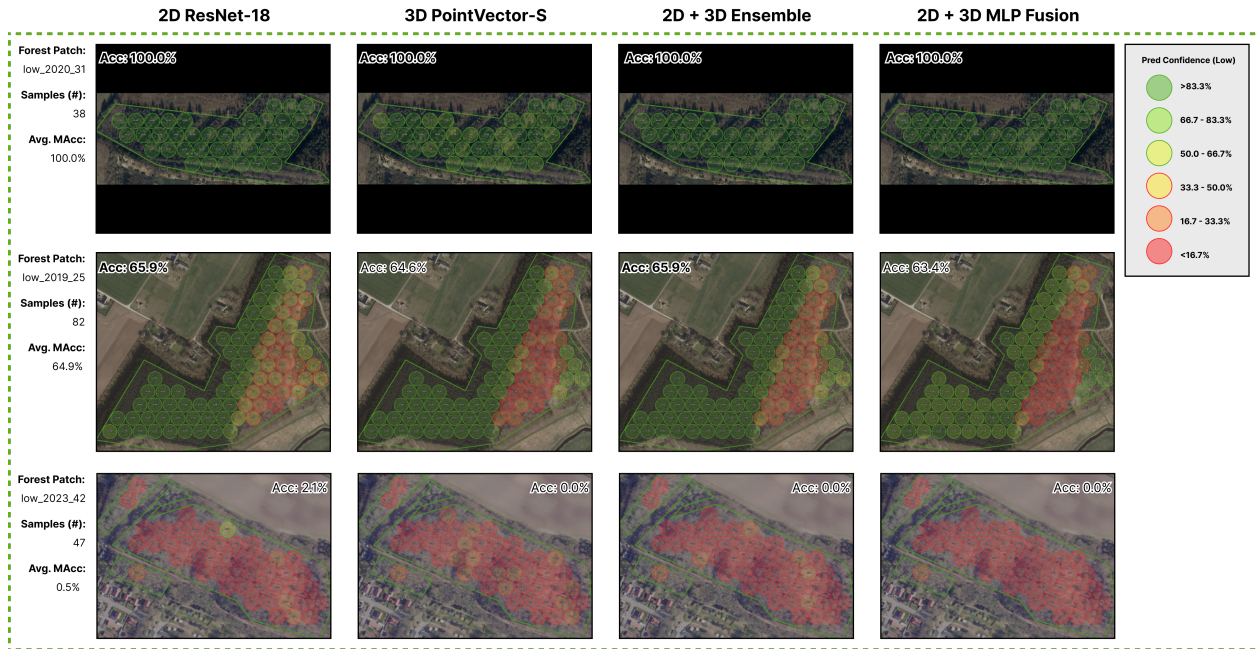


Figure B.11: Low biodiversity examples. Comparison of model predictions across three low biodiversity forest patches. Sample predictions shown with colored borders indicating classification outcome and confidence levels from all four models.

clearly distinguishable characteristics of high biodiversity potential. However, some patches (e.g., high_2021_21 and high_2021_27) showed consistently poor performance across all models, indicating that certain high biodiversity features may be difficult to distinguish using current remote sensing approaches.

We found similar patterns of variation in low biodiversity patches, where several patches (e.g., low_2020_31, low_2020_32) were classified perfectly by all models, while others (e.g., low_2023_42 through low_2023_45) proved particularly challenging with near-zero accuracy across all approaches. The MLP Fusion model showed notably strong performance on moderately difficult low biodiversity patches (e.g., low_2021_76, low_2022_42), often achieving the highest accuracy among all models.

We showcase the predictions on 3 high biodiversity potential forest patches and 3 low biodiversity potential forest patches in Figure B.10 and Figure B.11 respectively.

Table B.4: Forest Patch Analysis. Model performance comparison across forest patches in the test set. The table is divided into high- and low biodiversity potential forests, with each category showing the top 6, median 6 and bottom 6 forest patches sorted by average mean accuracy performance of all methods. For each forest patch, the mean accuracy is shown for all models, with the best performing model(s) highlighted in bold.

Forest Patch	Samples	Avg. MAcc	ResNet-18	PointVector-S	2D + 3D Ensemble	MLP Fusion
high_2019_50	72	100.0	100.0	100.0	100.0	100.0
high_2019_51	8	100.0	100.0	100.0	100.0	100.0
high_2019_52	58	100.0	100.0	100.0	100.0	100.0
high_2019_53	41	100.0	100.0	100.0	100.0	100.0
high_2019_54	80	100.0	100.0	100.0	100.0	100.0
high_2019_56	76	100.0	100.0	100.0	100.0	100.0
high_2019_66	147	96.1	93.2	95.9	96.6	98.6
high_2022_22	127	96.1	100.0	93.7	100.0	90.6
high_2021_22	57	96.1	100.0	94.7	96.5	93.0
high_2019_58	138	95.7	100.0	87.0	95.7	100.0
high_2019_65	201	94.8	93.5	99.0	98.5	88.1
high_2019_63	236	94.5	89.4	94.5	96.6	97.5
high_2019_62	50	44.0	100.0	2.0	16.0	58.0
high_2021_27	29	36.2	34.5	37.9	34.5	37.9
high_2021_24	216	29.3	77.3	7.9	22.7	9.3
high_2022_27	18	25.0	100.0	0.0	0.0	0.0
high_2022_28	5	25.0	100.0	0.0	0.0	0.0
high_2022_21	43	18.0	11.6	30.2	23.3	7.0
low_2020_31	38	100.0	100.0	100.0	100.0	100.0
low_2020_32	86	100.0	100.0	100.0	100.0	100.0
low_2021_60	13	100.0	100.0	100.0	100.0	100.0
low_2021_61	14	100.0	100.0	100.0	100.0	100.0
low_2022_36	29	100.0	100.0	100.0	100.0	100.0
low_2023_31	12	100.0	100.0	100.0	100.0	100.0
low_2022_42	49	79.1	49.0	89.8	81.6	95.9
low_2021_76	142	78.2	54.2	81.0	79.6	97.9
low_2021_57	34	76.5	64.7	79.4	76.5	85.3
low_2019_27	1	75.0	0.0	100.0	100.0	100.0
low_2022_34	69	71.0	34.8	91.3	78.3	79.7
low_2020_27	27	67.6	100.0	40.7	63.0	66.7
low_2021_64	90	3.1	1.1	5.6	3.3	2.2
low_2023_42	47	0.5	2.1	0.0	0.0	0.0
low_2023_29	7	0.0	0.0	0.0	0.0	0.0
low_2023_34	19	0.0	0.0	0.0	0.0	0.0
low_2023_38	26	0.0	0.0	0.0	0.0	0.0
low_2023_45	2	0.0	0.0	0.0	0.0	0.0

References

- Aerts, R., Honnay, O., 2011. Forest restoration, biodiversity and ecosystem functioning. *BMC Ecology* 11, 1–10. doi:10.1186/1472-6785-11-29.
- Alban, M., Nord-Larsen, T., R.-Nielsen, T., G. Cordius, J., O. Nielsen, A., Kudahl, T., Callesen, I., Vesterdal, L., B. Jørgensen, B., K. Johannsen, V., 2019. Skovstatistisk feltinstruks

- [Forest statistical field instructions]. Department of Geosciences and Natural Resource Management, Copenhagen University.
- Armeni, I., Sener, O., Zamir, A.R., Jiang, H., Brilakis, I., Fischer, M., Savarese, S., 2016. 3D semantic parsing of large-scale indoor spaces, in: *Computer Vision and Pattern Recognition (CVPR)*. doi:10.1109/CVPR.2016.170.
- Brandt, M., Chave, J., Li, S., Fensholt, R., and Jean-Pierre Wigneron, P.C., Gieseke, F., Saatchi, S., Tucker, C.J., Igel, C., 2024. High-resolution sensors and deep learning models for tree resource monitoring. *Nature Reviews Electrical Engineering* doi:10.1038/s44287-024-00116-8.
- Brandt, M., Rasmussen, K., Hiernaux, P., Herrmann, S., Tucker, C.J., Tong, X., Tian, F., Mertz, O., Kergoat, L., Mbow, C., David, J.L., Melocik, K.A., Dendoncker, M., Vincke, C., Fensholt, R., 2018. Reduction of tree cover in West African woodlands and promotion in semi-arid farmlands. *Nature Geoscience* 11, 328–333. doi:10.1038/s41561-018-0092-x.
- Cheng, Y., Oehmcke, S., Brandt, M., Rosenthal, L., Das, A., Vrieling, A., Saatchi, S., Wagner, F., Mugabowindekwe, M., Verbruggen, W., , Beier, C., Horion, S., 2024. Scattered tree death contributes to substantial forest loss in California. *Nature Communication* 15, 641. doi:10.1038/s41467-024-44991-z.
- Cui, Y., Chen, R., Chu, W., Chen, L., Tian, D., Li, Y., Cao, D., 2022. Deep learning for image and point cloud fusion in autonomous driving: A review. *IEEE Transactions on Intelligent Transportation Systems* 23. doi:10.1109/TITS.2020.3023541.
- Deng, X., Zhang, W., Ding, Q., Zhang, X., 2023. PointVector: A vector representation in point cloud analysis, in: *Computer Vision and Pattern Recognition (CVPR)*. doi:10.1109/CVPR52729.2023.00912.
- European Commission, 2020. EU Biodiversity Strategy for 2030: Bringing Nature Back Into Our Lives. Technical Report. European Commission.
- FAO, UNEP, 2020. The State of the World’s Forests 2020: Forests, Biodiversity and People. Technical Report. FAO and UNEP.

- GeoDanmark, 2024. Forårsbilleder ortofoto. <https://dataforsyningen.dk>. License: Creative Commons Attribution 4.0 International (CC BY 4.0).
- Goldstein, A., Turner, W., Spawn, S., Anderson-Teixeira, K.J., Cook-Patton, S., Fargione, J., Gibbs, H.K., Griscom, B., Hewson, J.H., Howard, J.F., Ledezma, J.C., Page, S., Koh, L.P., Rockström, J., Sanderman, J., Hole, D.G., 2020. Protecting irrecoverable carbon in Earth's ecosystems. *Nature Climate Change* 10, 287–295. doi:10.1038/s41558-020-0738-8.
- Hansen, H., Schrøder, L., Hvingel, L., Christiansen, J., 2011. Towards spatially enabled e-governance — a case study on SDI implementation. *International Journal of Spatial Data Infrastructures Research* 6, 73–96. doi:10.2902/1725-0463.2011.06.art4.
- Hansen, L., Jensen, S., Philipsen, M., Møgelmoose, A., Bodum, L., Moeslund, T., 2024. Open-Trench3D: A photogrammetric 3D point cloud dataset for semantic segmentation of underground utilities, in: *Computer Vision and Pattern Recognition Workshops (CVPRW)*.
- He, K., Zhang, X., Ren, S., Sun, J., 2015. Deep residual learning for image recognition, in: *Computer Vision and Pattern Recognition (CVPR)*. doi:10.1109/CVPR.2016.90.
- Jensen, S.B., Humblot-Renaux, G., Møgelmoose, A., Moeslund, T.B., 2023. Data-driven hyperparameter tuning for point-based 3D semantic segmentation, in: *IEEE International Conference on Image Processing Challenges and Workshops (ICIPCW)*. doi:10.1109/ICIPCW59416.2023.10328344.
- Johannsen, V.K., Rojas, S.K., Brunbjerg, A., Schumacher, J., Bladt, J., Karlsson Nyed, P., Moeslund, J., Nord-Larsen, T., Ejrnæs, R., 2015. Udvikling af et High Nature Value-HNV-skovkort for Danmark [Development of a High Nature Value - HNV forest map for Denmark]. Technical Report. Department of Geosciences and Natural Resource Management, Copenhagen University.
- Kangas, A., Astrup, R., Breidenbach, J., Fridman, J., Gobakken, T., Korhonen, K.T., Maltamo, M., Nilsson, M., Nord-Larsen, T., Næsset, E., Olsson, H., 2018. Remote sensing and forest inventories in Nordic countries – roadmap for the future. *Scandinavian Journal of Forest Research* 33, 397–412. doi:10.1080/02827581.2017.1416666.

- Kerry, R.G., Montalbo, F.J.P., Das, R., Patra, S., Mahapatra, G.P., Maurya, G.K., Nayak, V., Jena, A.B., Ukhurebor, K.E., Jena, R.C., Gouda, S., Majhi, S., Rout, J.R., 2022. An overview of remote monitoring methods in biodiversity conservation. *Environmental Science and Pollution Research International* 29, 80179–80221. doi:10.1007/s11356-022-23242-y.
- Klimadatastyrelsen, 2024. Danish height model. <https://dataforsyningen.dk>. License: Creative Commons Attribution 4.0 International (CC BY 4.0).
- Knapp, N., Fischer, R., Cazcarra-Bes, V., Huth, A., 2020. Structure metrics to generalize biomass estimation from lidar across forest types from different continents. *Remote Sensing of Environment* 237. doi:10.1016/j.rse.2019.111597.
- Kussul, N., Lavreniuk, M., Skakun, S., Shelestov, A., 2017. Deep learning classification of land cover and crop types using remote sensing data. *IEEE Geoscience and Remote Sensing Letters* 14, 778–782. doi:10.1109/LGRS.2017.2681128.
- LeCun, Y., Bengio, Y., Hinton, G., 2015. Deep learning. *Nature* 521, 436–444. doi:10.1038/nature14539.
- Li, S., Brandt, M., Fensholt, R., Kariryaa, A., Igel, C., Gieseke, F., Nord-Larsen, T., Oehmcke, S., Carlsen, A.H., Junttila, S., Tong, X., d’Aspremont, A., Ciais, P., 2023. Deep learning enables image-based tree counting, crown segmentation and height prediction at national scale. *PNAS Nexus* 2. doi:10.1093/pnasnexus/pgad076.
- Liu, S., Brandt, M., Nord-Larsen, T., Chave, J., Reiner, F., Lang, N., Tong, X., Ciais, P., Igel, C., Pascual, A., Guerra-Hernandez, J., Li, S., Mugabowindekwe, M., Saatchi, S., Yue, Y., Chen, Z., Fensholt, R., 2023. The overlooked contribution of trees outside forests to tree cover and woody biomass across Europe. *Science Advances* 9. doi:10.1126/sciadv.adh4097.
- Magnussen, S., Nord-Larsen, T., Riis-Nielsen, T., 2018. Lidar supported estimators of wood volume and aboveground biomass from the Danish national forest inventory (2012–2016). *Remote Sensing of Environment* 211, 146–153. doi:10.1016/j.rse.2018.04.015.

- Malhi, Y., Phillips, O., Lloyd, J., Baker, T., Wright, J., Almeida, S., Arroyo, L., Frederiksen, T., Grace, J., Higuchi, N., Killeen, T., Laurance, W., Leão, C., Lewis, S., Meir, P., Monteagudo, A., Neill, D., Núñez Vargas, P., Panfil, S., Patiño, S., Pitman, N., Quesada, C., Rudas-Ll., A., Salomão, R., Saleska, S., Silva, N., Silveira, M., Sombroek, W., Valencia, R., Vásquez Martínez, R., Vieira, I., Vinceti, B., 2002. An international network to monitor the structure, composition and dynamics of amazonian forests (RAINFOR). *Journal of Vegetation Science* 13, 439–450. doi:10.1111/j.1654-1103.2002.tb02068.x.
- Michel, A., Kirchner, T., Prescher, A.K., Schwärzel, K., 2022. Forest Condition in Europe: The 2022 Assessment. Technical Report. ICP Forests Technical Report.
- Nord-Larsen, T., J. Østergaard, M., Riis-Nielsen, T., Thomsen, I.M., Bentsen, N.S., B. Jørgensen, B., 2023. Skovstatistik 2022 [National Forest Inventory 2022]. Technical Report. Department of Geosciences and Natural Resource Management, Copenhagen University.
- Oehmcke, S., Li, L., Trepikli, K., Revenga, J.C., Nord-Larsen, T., Gieseke, F., Igel, C., 2024. Deep point cloud regression for above-ground forest biomass estimation from airborne lidar. *Remote Sensing of Environment* 302. doi:10.1016/j.rse.2023.113968.
- Pan, Y., Birdsey, R.A., Phillips, O.L., Jackson, R.B., 2013. The structure, distribution, and biomass of the world’s forests. *Annual Review of Ecology, Evolution, and Systematics* doi:10.1146/annurev-ecolsys-110512-135914.
- Potter, K., Conkling, B., 2022. Forest Health Monitoring: national status, trends, and analysis 2021. Technical Report. U.S. Department of Agriculture.
- QGIS Geographic Information System, 2024. URL: <https://www.qgis.org>.
- Qi, C.R., Yi, L., Su, H., Guibas, L.J., 2017. PointNet++: Deep hierarchical feature learning on point sets in a metric space, in: *Advances in Neural Information Processing Systems* (NeurIPS).
- Qian, G., Li, Y., Peng, H., Mai, J., Hammoud, H.A.A.K., Elhoseiny, M., Ghanem, B.,

2022. Pointnext: Revisiting PointNet++ with improved training and scaling strategies, in: *Advances in Neural Information Processing Systems (NeurIPS)*.
- Reiner, F., Brandt, M., Tong, X., Skole, D., Kariryaa, A., Ciaais, P., Davies, A., Hiernaux, P., Chave, J., Mugabowindekwe, M.M., Igel, C., Oehmcke, S., Gieseke, F., Li, M.S., Liu, S., Saatchi, S.S., Boucher, P., Singh, J., Taugourdeau, S., Dendoncker, M., Song, X.P., Mertz, O., Tucker, C., Fensholt, R., 2023. More than one quarter of Africa’s tree cover found outside areas previously classified as forest. *Nature Communication* 14. doi:10.1038/s41467-023-37880-4.
- Shi, S., Wang, X., Li, H., 2019. PointRCNN: 3D object proposal generation and detection from point cloud, in: *Computer Vision and Pattern Recognition (CVPR)*. doi:10.1109/CVPR.2019.00086.
- Thompson, I., Mackey, B., McNulty, S., Mosseler, A., 2009. Forest resilience, biodiversity, and climate change, in: *Secretariat of the Convention on Biological Diversity*.
- United Nations Department of Economic and Social Affairs, 2017. *The Sustainable Development Goals Report. Technical Report. United Nations*.
- United Nations Department of Economic and Social Affairs, 2021. *The Global Forest Goals Report 2021. Technical Report. United Nations*.
- Uy, M.A., Pham, Q.H., Hua, B.S., Nguyen, D.T., Yeung, S.K., 2019. Revisiting point cloud classification: A new benchmark dataset and classification model on real-world data, in: *International Conference on Computer Vision (ICCV)*. doi:10.1109/ICCV.2019.00167.
- Wolpert, D.H., 1992. Stacked generalization. *Neural Networks* 5, 241–259. doi:10.1016/S0893-6080(05)80023-1.
- Wu, H., Wen, C., Shi, S., Li, X., Wang, C., 2023. Virtual sparse convolution for multimodal 3D object detection, in: *Computer Vision and Pattern Recognition (CVPR)*. doi:10.1109/CVPR52729.2023.02074.

- Yang, Z., Sun, Y., Liu, S., Jia, J., 2020. 3DSSD: Point-based 3D single stage object detector, in: Computer Vision and Pattern Recognition (CVPR). doi:10.1109/CVPR42600.2020.01105.
- Yoo, J.H., Kim, Y., Kim, J., Choi, J.W., 2020. 3D-CVF: Generating joint camera and lidar features using cross-view spatial feature fusion for 3D object detection, in: European Conference on Computer Vision (ECCV). doi:10.1007/978-3-030-58583-9_43.
- Yuan, Q., Shen, H., Li, T., Li, Z., Li, S., Jiang, Y., Xu, H., Tan, W., Yang, Q., Wang, J., Gao, J., Zhang, L., 2020. Deep learning in environmental remote sensing: Achievements and challenges. Remote Sensing of Environment 241. doi:10.1016/j.rse.2020.111716.
- Zhang, L., Shao, Z., Liu, J., Cheng, Q., 2019. Deep learning based retrieval of forest aboveground biomass from combined LiDAR and Landsat 8 data. Remote Sensing 11. doi:10.3390/rs11121459.